

Transport approach to quantum state tomography

Jeanne Bourgeois^{1,2,3}, Gianmichele Blasi¹ and Géraldine Haack¹

¹*Department of Applied Physics, University of Geneva, 1211 Geneva, Switzerland*

²*Institute of Physics, Ecole Polytechnique Fédérale de Lausanne (EPFL), CH-1015 Lausanne, Switzerland*

³*Center for Quantum Science and Engineering, Ecole Polytechnique Fédérale de Lausanne (EPFL), CH-1015 Lausanne, Switzerland*

(Dated: September 15, 2025)

Quantum state tomography (QST) is a central task for quantum information processing, enabling quantum cryptography, computation, and state certification. Traditional QST relies on projective measurements of single- and two-qubit Pauli operators, requiring the system of interest to be isolated from environmental dissipation. In this work, we demonstrate that measuring currents and associated transport quantities flowing through a quantum system in an open configuration enable the reconstruction of its quantum state. This result relies on an exact relation between transport quantities and the Krylov subspaces associated with the Lindbladian which encodes the dynamical evolution of an open quantum system. We illustrate this transport approach to QST with the explicit example of a two-qubit system embedded in a two-terminal setup. As a direct consequence of our framework, we are able to provide a transport-based entanglement measure to certify the presence of quantum correlations, expressing the concurrence in terms of current averages and correlations function only. Our findings are analytical, providing fundamental insights into quantum information processing in open quantum systems. They establish new connections between the fields of mesoscopic physics and quantum information theory.

Introduction.— Demonstrating the presence of entanglement between multiple qubits is one of the key milestones for efficient quantum information processing, requiring the possibility to achieve quantum state tomography (QST) of multi-partite systems [1–3]. Seminal experimental works based on different platforms have realized QST involving one to multiple qubits, with superconducting platforms [4, 5], trapped ions [6, 7] and Nitrogen-vacancy centers [8, 9]. QST protocols are typically based on linear inversion of local and global Pauli observables directly related to elements of the density operator, and on numerical optimization through various statistical estimators [10, 11] or classical shadow algorithms [12]. Remarkably, QST protocols contributed very recently to demonstrate loophole-free violation of Bell inequalities using solid-state qubits [13–15], and are starting to be explored from the point of view of novel advanced numerical techniques [16].

While uncontrolled dissipation leading to noise is considered as detrimental in the above experimental achievements, its role towards quantum information processing and its applications has considerably changed in the past two decades. On one hand, engineered dissipation has been shown to constitute an alternative lever for generating and manipulating quantum resources, through stabilization of entangled states in decoherence-free subspaces [17–21] and autonomous quantum error correction codes [22–24]. On the other hand, it remains an open question whether uncontrolled dissipation, in the form of heat from a thermodynamic point of view, can also constitute a resource for quantum information processing. As a consequence, several theoretical proposals for autonomous generation of entanglement in open quantum systems se-

tups have followed [25–32]. In particular, the successful functioning of an entanglement engine was shown to be conditioned on a minimal critical charge or heat current flowing through two interacting qubits in a two-terminal device [33–35]. This result paved the way for exploiting heat as a witness of entanglement, an approach that was generalized to quantum properties in [36]. All these contributions suggested a connection between transport properties in an open quantum system and its quantum state.

In this work, we provide an affirmative answer to the fundamental question whether transport measurements, in the form of current averages and fluctuations, can provide a complete characterization of the state of an open quantum system. We derive exact relations between transport quantities - currents, time-derivatives of the currents, and current correlation functions - and density operator's elements. We show that these relations originate from the Krylov subspaces of the populations of the system generated by the Lindbladian superoperator of the open quantum system. This provides a general theoretical framework and a fundamental understanding of the underlying principles behind a transport approach to QST. We illustrate these findings with a complete analytical description of two interacting qubits weakly coupled to two Markovian reservoirs, their dynamics being assessed within a master equation approach. We show that this transport-based tomography scheme only requires the *a priori* knowledge of the system-bath coupling strengths. All other parameters, including those governing the system's unitary dynamics and local pure dephasing, can be extracted from additional transport-based quantities. Importantly, these results

allow us to express the concurrence, an entanglement measure, in terms of transport quantities only. This further establishes fundamental connections between the quantum state of an open quantum system and observables measured in the environment.

Theoretical framework.— We consider an open quantum system made of N interacting qubits, whose internal dynamics is set by the Lindbladian \mathcal{L}_S . Additionally, we assume $M \leq N$ qubits to be locally coupled to Markovian thermal baths through single-particle tunneling-type interaction Hamiltonians. These reservoirs are biased in voltage and temperature such that charge and heat currents flow through the system. Assuming weak system-bath coupling compared to the typical energy scales of the multi-qubit system, the dynamics of the corresponding reduced density operator $\hat{\rho}$ is accurately captured by a local Lindblad master equation of the form [33, 37–40] ($\hbar = k_B = 1$ throughout the work):

$$\dot{\hat{\rho}} = \mathcal{L}\hat{\rho} = \mathcal{L}_S\hat{\rho} + \sum_{j=1}^M (\gamma_j^+ \mathcal{D}[\hat{\sigma}_+^{(j)}] + \gamma_j^- \mathcal{D}[\hat{\sigma}_-^{(j)}])\hat{\rho}, \quad (1)$$

where $\mathcal{D}[A] \bullet \equiv A \bullet A^\dagger - (A^\dagger A \bullet + \bullet A^\dagger A)/2$ is the dissipator, $\hat{\sigma}_+^{(j)}$ ($\hat{\sigma}_-^{(j)}$) the raising (lowering) operators for qubit j and γ_j^+ (γ_j^-) the rate of particles tunneling in (out) of the system from (to) reservoir j (details on our analytical method are provided in the Supp. Mat. [41]). The second term in the right-hand-side expression captures the dissipative dynamics induced by the thermal baths, including relaxation and loss of quantum coherence.

Assuming the validity of Eq. (29), the super-operators $\mathcal{I}_j \bullet \equiv \gamma_j^+ \hat{\sigma}_+^{(j)} \bullet \hat{\sigma}_-^{(j)} - \gamma_j^- \hat{\sigma}_-^{(j)} \bullet \hat{\sigma}_+^{(j)}$ enable the calculation of the current operators' averages and higher-order moments, noted below with the compact notation $I_P(t) \equiv \text{Tr}[\prod_{j \in P} \mathcal{I}_j \hat{\rho}(t)]$ for $P \subseteq \{1, \dots, M\}$. The case $P = \{j\}$ corresponds to the averaged current from reservoir j into the system, while $P = \{i, j\}$ provides the instantaneous current cross-correlations between the leads i and j [43]. The k -th time derivative of the current moment $I_P^{(k)}(t)$ is given by

$$I_P^{(k)}(t) = \text{Tr} \left[\prod_{j \in P} \mathcal{I}_j \mathcal{L}^k \hat{\rho}(t) \right]. \quad (2)$$

Of importance for our main result formulated below, the time evolution of any initial state $\hat{\rho}_0$ is governed by the propagator $e^{\mathcal{L}t}$, such that $\hat{\rho}(t) = e^{\mathcal{L}t} \hat{\rho}_0$. This implies that the state $\hat{\rho}(t)$ remains confined to the subspace generated by successive applications of the Lindbladian to the initial state, namely the set $\{\mathcal{L}^k \hat{\rho}_0\}_{k=0}^\infty$, referred to as the *Krylov space* associated with the Lindbladian \mathcal{L} and the state $\hat{\rho}_0$ [44]. Equivalently, in the Heisenberg picture the time evolution of an operator \hat{u}_0 is confined

to the Krylov subspace spanned by the set of operators $\{\mathcal{L}^{\dagger k} \hat{u}_0\}_{k=0}^\infty$. In practice, an orthonormal basis for the Krylov space can be constructed using the Arnoldi algorithm [45, 46]: after K iterations, the algorithm generates orthonormal vectors that span $\{\mathcal{L}^k \hat{\rho}_0\}_{k=0}^{K-1}$ in the Schrödinger picture, or $\{\mathcal{L}^{\dagger k} \hat{u}_0\}_{k=0}^{K-1}$ in the Heisenberg picture, providing a reduced K -dimensional subspace in which the time evolution can be efficiently computed.

Main result.— The fundamental result behind our proposal for a transport approach to QST lies in the connection between transport quantities and the elements of the system's density operator $\hat{\rho}$ projected onto suitable Krylov subspaces. This connection arises when considering Krylov spaces generated by the operators:

$$\hat{n}_P = \prod_{j \in P} \hat{n}_j, \quad P \subseteq \{1, \dots, M\}, \quad (3)$$

where \hat{n}_j is the occupation-number projector of qubit j coupled to a thermal reservoir. The resulting sum of Krylov subspaces can be written as

$$\mathcal{K} = \sum_{P \subseteq \{1, \dots, M\}} \mathcal{K}_P, \quad \mathcal{K}_P = \text{span}\{\mathcal{L}^{\dagger k} \hat{n}_P \mid k \in \mathbb{N}\}. \quad (4)$$

Here the sum runs over all subsets P of qubit-reservoir indices, and each \mathcal{K}_P contains the repeated actions of \mathcal{L}^\dagger on the corresponding projector \hat{n}_P .

Elements of the density operator of the system are obtained by projecting it onto the vectors of the Krylov spaces:

$$p_{P,k} \equiv \langle \mathcal{L}^{k\dagger} \hat{n}_P, \hat{\rho}(t) \rangle = \text{Tr}[\hat{n}_P \mathcal{L}^k \hat{\rho}(t)], \quad (5)$$

where the notation $\langle \cdot, \cdot \rangle$ corresponds to Hilbert-Schmidt inner product of two operators \hat{A} and \hat{B} , $\langle \hat{A}, \hat{B} \rangle = \text{Tr}[\hat{A}^\dagger \hat{B}]$. Physically, these elements correspond to the occupation numbers $p_{P,0}(t) = \langle \hat{n}_P \rangle(t) \equiv n_P(t)$ ($k = 0$), and their high-order time-derivatives $p_{P,k}(t) = n_P^{(k)}(t)$ ($k \geq 1$).

The elements $p_{P,k}$ of Eq. (5) are related to the k -th derivative of the current moments $I_{P'(t)}$ defined in Eq. (2) through the identity:

$$p_{P,k} = \text{Tr} \left[\left(\prod_{j \in P} \frac{\gamma_j^+ - \mathcal{I}_j}{\Gamma_j} \right) \mathcal{L}^k \hat{\rho}(t) \right] \quad (6)$$

$$= \sum_{P' \subseteq P} \left(\prod_{i \notin P', j \in P} \frac{\gamma_i^+}{\Gamma_j} \right) (-1)^{|P'|} I_{P'}^{(k)}(t), \quad (7)$$

with $\Gamma_j \equiv \gamma_j^+ + \gamma_j^-$, the index P' running through the list of all subsets of P , i through the list of indices in P not in P' and j through all P . The proof of this identity, a fundamental and technical result of this work, is provided in the End Matter.

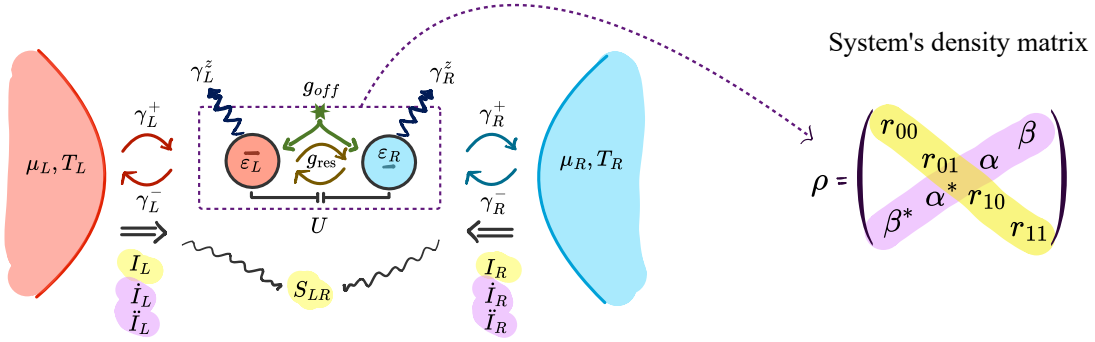


FIG. 1. Illustration of the tomography of a two-qubit open quantum system through the measurement of transport observables. The represented evolution corresponds to Eq. (10).

Whether this quantum tomography protocol is complete or not depends on the size of the Krylov spaces with respect to the one of the Hilbert space \mathcal{H} of the system. In general, $\dim(\mathcal{K}_P) \leq \dim(\mathcal{H})$ [44], requiring the combination of several Krylov spaces, corresponding to different occupation-number operators, to potentially achieve complete QST. We emphasize that the size of the Krylov subspaces depends on the spectral properties of the Lindbladian, as analyzed in the Supp. Mat. [41]. For the explicit example of two-qubit state tomography discussed below, we show that complete QST can be achieved by combining Krylov spaces associated to different occupation-number operators.

Two-qubit quantum state tomography.— We illustrate the transport approach to QST with the paradigmatic example of a two-qubit system coupled to two reservoirs, see Figure 1. We write the density matrix in the Fock basis $\{|00\rangle, |01\rangle, |10\rangle, |11\rangle\}$ as

$$\hat{\rho} = \begin{pmatrix} r_{00} & v & x & \beta \\ v^* & r_{01} & \alpha & y \\ x^* & \alpha^* & r_{10} & z \\ \beta^* & y^* & z^* & r_{11} \end{pmatrix} \quad (8)$$

with the diagonal elements corresponding to populations (real numbers) and off-diagonal elements to coherences (complex numbers). The two qubit-reservoir pairs are referred to as “left” (L) and “right” (R).

Without any prior knowledge of the internal evolution of the two-qubit system, the application of Eq. (7) for $k = 0$ to the population projectors \hat{n}_L , \hat{n}_R and $\hat{n}_L \hat{n}_R$ allows us to determine the populations of the system via the left and right currents $I_L(t)$ and $I_R(t)$ and their instantaneous cross-correlation function $S_{LR}(t) =$

$$I_{LR}(t) - I_L(t)I_R(t):$$

$$r_{01}(t) = -\frac{S_{LR}(t)}{\Gamma_L \Gamma_R} - \frac{I_R(t) - \gamma_R^+ I_L(t) + \gamma_L^-}{\Gamma_R}, \quad (9a)$$

$$r_{10}(t) = -\frac{S_{LR}(t)}{\Gamma_L \Gamma_R} - \frac{I_L(t) - \gamma_L^+ I_R(t) + \gamma_R^-}{\Gamma_L}, \quad (9b)$$

$$r_{11}(t) = \frac{S_{LR}(t)}{\Gamma_L \Gamma_R} + \frac{I_L(t) - \gamma_L^+ I_R(t) - \gamma_R^+}{\Gamma_L \Gamma_R}, \quad (9c)$$

with $r_{00}(t)$ being reconstructed from the trace property $\text{Tr}\{\hat{\rho}(t)\} = 1$. Details of this derivation are provided in the End Matter. The set of equations (66) attests that average currents and cross-correlated noise are sufficient to determine the populations of a two-qubit system at any given time, given that the couplings $\gamma_{L/R}^\pm$ are known *a priori*. This assumption is consistent with state-of-the-art experimental setups, as discussed in the conclusion of this work. Interestingly, although the presence of baths influences the evolution of all elements of the density matrix, the current quantities $I_L(t)$, $I_R(t)$ and $S_{LR}(t)$ at a fixed time t depend solely on the populations $r_{ij}(t)$ and not on the coherences.

To access the coherences, we make use of Eqs. (6) and (7) with $k = 1$ and $k = 2$. The corresponding equations then depend on the system’s internal evolution. In the following, we consider it to be given by the Lindbladian

$$\mathcal{L}_S \bullet = -i[\hat{H}_S, \bullet] + \sum_{j=L,R} \frac{\gamma_j^z}{2} \mathcal{D}[\hat{\sigma}_z^{(j)}] \bullet \quad (10)$$

with H_S a generic two-qubit Hamiltonian that induces a coupled dynamics for the diagonal and off-diagonal elements of $\hat{\rho}$,

$$\hat{H}_S = \varepsilon_L \hat{n}_L + \varepsilon_R \hat{n}_R + U \hat{n}_L \hat{n}_R + (g_{\text{res}} \hat{\sigma}_+^{(L)} \hat{\sigma}_-^{(R)} + g_{\text{off}} \hat{\sigma}_+^{(L)} \hat{\sigma}_+^{(R)}) + h.c.. \quad (11)$$

The energies $\varepsilon_{L/R}$ set the bare energies of the qubits L/R, the energy U captures on-site interactions (like Coulomb interactions for charge qubits), while the energies g_{res} and

Case	Populations	Transport quantities	Transport parameters
	r_{00}, r_{01}, r_{10}	I_L, I_R, S_{LR}	$\gamma_L^\pm, \gamma_R^\pm$

Case	Generated coherences	Additional transport quantities	Hamiltonian param. & add. measurement when Γ_z unknown
	α, β	\dot{I}_L, \ddot{I}_L and \dot{I}_R, \ddot{I}_R	$g_{\text{res}}, g_{\text{off}}, \delta, E$ or $I_L^{(3)} \text{ or } I_R^{(3)}$
$\delta = 0$ $E = 0$	$\text{Im}(\alpha), \text{Im}(\beta)$	\dot{I}_L and \dot{I}_R	$g_{\text{res}}, g_{\text{off}}$ or \emptyset
$g_{\text{off}} = 0$	$\text{Im}(\alpha), \text{Re}(\alpha)$	\dot{I}_L, \ddot{I}_L or \dot{I}_R, \ddot{I}_R	g_{res}, δ or $I_L^{(3)} \text{ or } I_R^{(3)}$

TABLE I. Table summarizing which transport quantities allow for the reconstruction of the populations and the coherences of the two-qubit system. The rightmost column lists the transport and Hamiltonian parameters which *a priori* knowledge is required to achieve QST. If certain parameters are not known (for example here, dephasing rate $\Gamma_z = \gamma_L^z + \gamma_R^z$), we list additional transport quantities that can be exploited to assess them (see Supp. Mat. for details). The general case (no specific assumption) corresponds to Eq. (11).

g_{off} set resonant (particle-conserving) and off-resonant (particle-non-conserving) interactions respectively and are supposed real without loss of generality. The dissipative terms of the Lindbladian \mathcal{L}_S (10), involving the z-Pauli jump operators $\dot{\sigma}_z^{(\alpha)}$ and proportional to rates $\gamma_z^{(\alpha)}$, capture pure dephasing processes contributing to the finite coherence time of the qubits.

Given this internal evolution and applying Eq. (7) for $P = \{L\}, \{R\}$ and $k = 1, 2$, the first time-derivatives of the left and right currents, $\dot{I}_L(t)$ and $\dot{I}_R(t)$, determine the imaginary part of the coherences α and β ,

$$-4g_{\text{res}} \text{Im} \alpha(t) = \frac{\dot{I}_L(t)}{\Gamma_L} + I_L(t) - \frac{\dot{I}_R(t)}{\Gamma_R} - I_R(t), \quad (12a)$$

$$-4g_{\text{off}} \text{Im} \beta(t) = \frac{\dot{I}_L(t)}{\Gamma_L} + I_L(t) + \frac{\dot{I}_R(t)}{\Gamma_R} + I_R(t) \quad (12b)$$

while further measuring their second time-derivatives, $\ddot{I}_L(t)$ and $\ddot{I}_R(t)$, yields the real part of α and β (see End Matter for details).

Higher time-derivatives of the currents, as well as time-derivatives of the cross-correlation function, only add redundant information on the density matrix. In other words, $\mathcal{L}^{\dagger k} \hat{n}_j$ for $j = L, R$ and $k = 0, 1, 3$, in addition to $\hat{n}_L \hat{n}_R$, generate the full subspace \mathcal{K} defined in Eq. (4). Interestingly, the set of accessible coherences depends on the evolution properties of the system, and exactly corresponds to the coherences being non-zero in the steady-state regime. In Table I, we summarize the features of the transport approach to two-qubit QST for specific cases of the Hamiltonian H_S in Eq. (11). Additional transport measurements may nonetheless be exploited to probe the system's evolution (see Supp. Mat. [41]).

More generally, accessing all density matrix's elements is possible, but it requires a Hamiltonian involving additional operators. In the Supp. Mat., we provide a demonstration of this generalization towards complete QST [41].

Steady-state regime.— This transport approach to QST is particularly advantageous in the steady state (*ss*), where all time derivatives vanish. For all $P \subseteq \{1, \dots, M\}$, the identity given by Eq. (7) then reduces to:

$$p_{P,0}^{(ss)} = \sum_{P' \subseteq P} \left(\prod_{i \notin P', j \in P} \frac{\gamma_i^+}{\Gamma_j} \right) (-1)^{|P'|} I_{P'}^{(ss)}, \quad (13a)$$

$$p_{P,k}^{(ss)} = 0 \quad \text{for } k \geq 1. \quad (13b)$$

In the illustrative case of the two-qubit system, the populations and coherences are simply accessed by the measurements of steady-state currents and noise, as shown in the End Matter.

Transport-based entanglement measures.— Remarkably, our demonstration of complete transport-based QST allows us to express entanglement measures in terms of currents and associated quantities only. While the concurrence is defined from the Schmidt coefficients [47], it takes a particular simple form for X-shaped density matrices of two-qubit systems [48]: $\mathcal{C} = 2 \max\{0, |\alpha| - \sqrt{r_{00}r_{11}}, |\beta| - \sqrt{r_{01}r_{10}}\}$. In the illustrative case of two energy-degenerate qubits ($\delta = 0$) with resonant interaction only ($g_{\text{off}} = 0$), initialized in their ground state, the density matrix $\rho(t)$ remains X-shaped at all time t and its concurrence can then be expressed as:

$$\mathcal{C} = \max \left\{ 0, \left| \frac{1}{g_{\text{res}}} \left(\frac{\dot{I}_L}{\Gamma_L} + I_L \right) \right| - 2 \sqrt{\left(\frac{S_{LR}}{\Gamma_L \Gamma_R} + \frac{I_L - \gamma_L^+ I_R - \gamma_R^+}{\Gamma_L} \right) \left(\frac{S_{LR}}{\Gamma_L \Gamma_R} + \frac{I_L + \gamma_L^- I_R + \gamma_R^-}{\Gamma_R} \right)} \right\}. \quad (14)$$

Equation (14) shows that certifying the presence of

entanglement in an open quantum system does not

require QST through decoupling the system from its environments and performing projective measurements. In the Supp. Mat. [41], we provide the expression of the concurrence \mathcal{C} in the general case. These results formally connect entanglement measures of a quantum system and transport quantities accessible in an open device configuration.

Experimental relevance and conclusion.— Transport-based QST relies on the measurement of time-resolved current traces, particle or charge currents. For emblematic quantum transport setups with solid-state qubits like quantum dots, current traces correspond to projective measurements of incoming charges into metallic contacts. Repetition of these measurements enable access to averaged time-resolved current traces of interest to our approach, see the reviews [49, 50].

Another experimental aspect that is central to our approach concerns the knowledge of the system dynamics and the system–bath coupling strengths. Although our method relies on this prior information, this does not represent a limitation: the coupling strengths can be accurately determined with state-of-the-art spectroscopy measurements in solid-state platforms [51–54], while recent experiments on hybrid setups have demonstrated that the system dynamics and possible dephasing can also be estimated. Crucially, we show in the Supp. Mat. [41] that our transport-based approach itself provides access to these parameters: by measuring current derivatives at different times, one can directly infer the system’s internal dynamics and dissipation rates. Therefore, such a necessary knowledge does not constitute a limitation to the applicability of our proposal.

This work is a significant step towards demonstrating complete QST of a quantum system from measuring out-of-equilibrium environments and associated transport properties. We provide a general theoretical framework based on the concept of Krylov subspaces generated by the Lindbladian to prove the validity of this approach. We illustrate it with the specific case of two qubits embedded into a two-terminal device. This work paves the way to quantum information processing in out-of-equilibrium quantum devices. This is of particular interest towards error mitigation [55] and neuromorphic computing [56–58].

Acknowledgements.— We are thankful for fruitful discussions with Landry Bretheau, Gwendal Fèvre and Matteo Secli, and useful feedbacks from Vincenzo Savona. All authors acknowledge the support of NCCR SwissMAP.

[1] M. Paris and J. Řeháček, eds., *Quantum State Estimation* (Springer Berlin Heidelberg, 2004).

[2] M. A. Nielsen and I. L. Chuang, *Quantum Computation and Quantum Information: 10th Anniversary Edition* (Cambridge University Press, 2012).

[3] K. Vogel and H. Risken, Determination of quasiprobability distributions in terms of probability distributions for the rotated quadrature phase, *Physical Review A* **40**, 2847–2849 (1989).

[4] S. Filipp, P. Maurer, P. J. Leek, M. Baur, R. Bianchetti, J. M. Fink, M. Göppl, L. Steffen, J. M. Gambetta, A. Blais, and A. Wallraff, Two-qubit state tomography using a joint dispersive readout, *Physical Review Letters* **102**, 10.1103/physrevlett.102.200402 (2009).

[5] R. Bianchetti, S. Filipp, M. Baur, J. M. Fink, C. Lang, L. Steffen, M. Boissonneault, A. Blais, and A. Wallraff, Control and tomography of a three level superconducting artificial atom, *Physical Review Letters* **105**, 10.1103/physrevlett.105.223601 (2010).

[6] C. F. Roos, G. P. T. Lancaster, M. Riebe, H. Häffner, W. Hänsel, S. Gulde, C. Becher, J. Eschner, F. Schmidt-Kaler, and R. Blatt, Bell states of atoms with ultra-long lifetimes and their tomographic state analysis, *Physical Review Letters* **92**, 10.1103/physrevlett.92.220402 (2004).

[7] H. Häffner, W. Hänsel, C. F. Roos, J. Benhelm, D. Chekalakar, M. Chwalla, T. Körber, U. D. Rapol, M. Riebe, P. O. Schmidt, C. Becher, O. Gühne, W. Dür, and R. Blatt, Scalable multiparticle entanglement of trapped ions, *Nature* **438**, 643–646 (2005).

[8] G. M. Leskowitz and L. J. Mueller, State interrogation in nuclear magnetic resonance quantum-information processing, *Physical Review A* **69**, 10.1103/physreva.69.052302 (2004).

[9] J. Wrachtrup and F. Jelezko, Processing quantum information in diamond, *Journal of Physics: Condensed Matter* **18**, S807–S824 (2006).

[10] D. F. V. James, P. G. Kwiat, W. J. Munro, and A. G. White, Measurement of qubits, *Physical Review A* **64**, 10.1103/physreva.64.052312 (2001).

[11] K. Bartkiewicz, A. Černoch, K. Lemr, and A. Miranowicz, Priority choice experimental two-qubit tomography: Measuring one by one all elements of density matrices, *Scientific Reports* **6**, 10.1038/srep19610 (2016).

[12] H.-Y. Huang, R. Kueng, and J. Preskill, Predicting many properties of a quantum system from very few measurements, *Nature Physics* **16**, 1050–1057 (2020).

[13] K. Thapliyal, S. Banerjee, and A. Pathak, Tomograms for open quantum systems: In(finite) dimensional optical and spin systems, *Annals of Physics* **366**, 148–167 (2016).

[14] P. Kurpiers, P. Magnard, T. Walter, B. Royer, M. Pechal, J. Heinsoo, Y. Salathé, A. Akin, S. Storz, J.-C. Besse, S. Gasparinetti, A. Blais, and A. Wallraff, Deterministic quantum state transfer and remote entanglement using microwave photons, *Nature* **558**, 264–267 (2018).

[15] S. Storz, J. Schär, A. Kulikov, P. Magnard, P. Kurpiers, J. Lütolf, T. Walter, A. Copetudo, K. Reuer, A. Akin, J.-C. Besse, M. Gabureac, G. J. Norris, A. Rosario, F. Martin, J. Martinez, W. Amaya, M. W. Mitchell, C. Abellán, J.-D. Bancal, N. Sangouard, B. Royer, A. Blais, and A. Wallraff, Loophole-free bell inequality violation with superconducting circuits, *Nature* **617**, 265–270 (2023).

[16] G. Torlai, G. Mazzola, J. Carrasquilla, M. Troyer, R. Melko, and G. Carleo, Neural-network quantum state tomography, *Nature Physics* **14**, 447–450 (2018).

[17] D. A. Lidar, I. L. Chuang, and K. B. Whaley,

Decoherence-free subspaces for quantum computation, *Physical Review Letters* **81**, 2594–2597 (1998).

[18] P. G. Kwiat, A. J. Berglund, J. B. Altepeter, and A. G. White, Experimental verification of decoherence-free subspaces, *Science* **290**, 498–501 (2000).

[19] D. Kielpinski, V. Meyer, M. A. Rowe, C. A. Sackett, W. M. Itano, C. Monroe, and D. J. Wineland, A decoherence-free quantum memory using trapped ions, *Science* **291**, 1013–1015 (2001).

[20] D. Kielpinski, C. Monroe, and D. J. Wineland, Architecture for a large-scale ion-trap quantum computer, *Nature* **417**, 709–711 (2002).

[21] Z. J. Deng, M. Feng, and K. L. Gao, Preparation of entangled states of four remote atomic qubits in decoherence-free subspace, *Physical Review A* **75**, 10.1103/physreva.75.024302 (2007).

[22] F. Reiter, A. S. Sørensen, P. Zoller, and C. A. Muschik, Dissipative quantum error correction and application to quantum sensing with trapped ions, *Nature Communications* **8**, 10.1038/s41467-017-01895-5 (2017).

[23] Q. Xu, G. Zheng, Y.-X. Wang, P. Zoller, A. A. Clerk, and L. Jiang, Autonomous quantum error correction and fault-tolerant quantum computation with squeezed cat qubits, *npj Quantum Information* **9**, 10.1038/s41534-023-00746-0 (2023).

[24] T. Hillmann and F. Quijandría, Quantum error correction with dissipatively stabilized squeezed-cat qubits, *Physical Review A* **107**, 10.1103/physreva.107.032423 (2023).

[25] V. Eisler and Z. Zimborás, Entanglement in the xxspin chain with an energy current, *Physical Review A* **71**, 10.1103/physreva.71.042318 (2005).

[26] L. Hartmann, W. Dür, and H. J. Briegel, Entanglement and its dynamics in open, dissipative systems, *New Journal of Physics* **9**, 230–230 (2007).

[27] L. Quiroga, F. J. Rodríguez, M. E. Ramírez, and R. París, Nonequilibrium thermal entanglement, *Physical Review A* **75**, 10.1103/physreva.75.032308 (2007).

[28] B. Bellomo and M. Antezza, Creation and protection of entanglement in systems out of thermal equilibrium, *New Journal of Physics* **15**, 113052 (2013).

[29] J. Bohr Brask, G. Haack, N. Brunner, and M. Huber, Autonomous quantum thermal machine for generating steady-state entanglement, *New Journal of Physics* **17**, 113029 (2015).

[30] A. Hewgill, A. Ferraro, and G. De Chiara, Quantum correlations and thermodynamic performances of two-qubit engines with local and common baths, *Physical Review A* **98**, 10.1103/physreva.98.042102 (2018).

[31] A. Das, A. A. Khan, S. D. Mishra, P. Solanki, B. De, B. Muralidharan, and S. Vinjanampathy, Steady-state tunable entanglement thermal machine using quantum dots, *Quantum Science and Technology* **7**, 045034 (2022).

[32] S. Khandelwal, B. Annby-Andersson, G. F. Diotallevi, A. Wacker, and A. Tavakoli, *Maximal steady-state entanglement in autonomous quantum thermal machines* (2024).

[33] S. Khandelwal, N. Palazzo, N. Brunner, and G. Haack, Critical heat current for operating an entanglement engine, *New Journal of Physics* **22**, 073039 (2020).

[34] D. Farina, B. Benazout, F. Centrone, and A. Acin, *Thermodynamic precision in the nonequilibrium exchange scenario* (2023).

[35] G. Francesco Diotallevi, B. Annby-Andersson, P. Samuelsson, A. Tavakoli, and P. Bakhshinezhad, Steady-state entanglement production in a quantum thermal machine with continuous feedback control, *New Journal of Physics* **26**, 053005 (2024).

[36] A. de Oliveira Junior, J. B. Brask, and P. Lipka-Bartosik, Heat as a witness of quantum properties, *Physical Review Letters* **134**, 10.1103/physrevlett.134.050401 (2025).

[37] H.-P. Breuer and F. Petruccione, *The Theory of Open Quantum Systems* (Oxford University PressOxford, 2007).

[38] G. Schaller, Dynamics of open quantum systems, in *Open Quantum Systems Far from Equilibrium* (Springer International Publishing, 2014) p. 1–26.

[39] P. P. Hofer, M. Perarnau-Llobet, L. D. M. Miranda, G. Haack, R. Silva, J. B. Brask, and N. Brunner, Markovian master equations for quantum thermal machines: local versus global approach, *New Journal of Physics* **19**, 123037 (2017).

[40] G. T. Landi, M. J. Kewming, M. T. Mitchison, and P. P. Potts, Current fluctuations in open quantum systems: Bridging the gap between quantum continuous measurements and full counting statistics, *PRX Quantum* **5**, 10.1103/prxquantum.5.020201 (2024).

[41] See Supplementary Material for the transport approach to two-qubit quantum state tomography, which includes Refs. [33, 37–40, 42, 43, 45, 46, 59–63].

[42] M. Cattaneo, G. L. Giorgi, S. Maniscalco, and R. Zambrini, Local versus global master equation with common and separate baths: superiority of the global approach in partial secular approximation, *New Journal of Physics* **21**, 113045 (2019).

[43] G. Blasi, S. Khandelwal, and G. Haack, Exact finite-time correlation functions for multiterminal setups: Connecting theoretical frameworks for quantum transport and thermodynamics, *Physical Review Research* **6**, 10.1103/physrevresearch.6.043091 (2024).

[44] P. Nandy, A. S. Matsoukas-Roubeas, P. Martínez-Azcona, A. Dymarsky, and A. del Campo, Quantum dynamics in krylov space: Methods and applications, *Physics Reports* **1125-1128**, 1 (2025).

[45] W. E. Arnoldi, The principle of minimized iterations in the solution of the matrix eigenvalue problem, *Quart. Appl. Math.* **9** (1951).

[46] A. Bhattacharya, P. Nandy, P. P. Nath, and H. Sahu, Operator growth and krylov construction in dissipative open quantum systems, *Journal of High Energy Physics* **2022**, 10.1007/JHEP12(2022)081 (2022).

[47] W. K. Wootters, Entanglement of formation of an arbitrary state of two qubits, *Physical Review Letters* **80**, 2245–2248 (1998).

[48] T. Yu and J. Eberly, Evolution from entanglement to decoherence, *Quantum Information and Computation* **7**, 459–468 (2007).

[49] L. P. Kouwenhoven, C. M. Marcus, P. L. McEuen, S. Tarucha, R. M. Westervelt, and N. S. Wingreen, Electron transport in quantum dots, in *Mesoscopic Electron Transport* (Springer Netherlands, 1997) p. 105–214.

[50] W. G. van der Wiel, S. De Franceschi, J. M. Elzerman, T. Fujisawa, S. Tarucha, and L. P. Kouwenhoven, Electron transport through double quantum dots, *Reviews of Modern Physics* **75**, 1–22 (2002).

[51] Y.-Y. Liu, K. Petersson, J. Stehlik, J. Taylor, and J. Petta, Photon emission from a cavity-coupled double quantum dot, *Physical Review Letters* **113**,

10.1103/physrevlett.113.036801 (2014).

[52] A. Stockklauser, P. Scarlino, J. Koski, S. Gasparinetti, C. Andersen, C. Reichl, W. Wegscheider, T. Ihn, K. Ensslin, and A. Wallraff, Strong coupling cavity qed with gate-defined double quantum dots enabled by a high impedance resonator, *Physical Review X* **7**, 10.1103/physrevx.7.011030 (2017).

[53] Y. Wang, Y. Chen, H. T. Bui, C. Wolf, M. Haze, C. Mier, J. Kim, D.-J. Choi, C. P. Lutz, Y. Bae, S.-h. Phark, and A. J. Heinrich, An atomic-scale multi-qubit platform, *Science* **382**, 87–92 (2023).

[54] H. Duprez, S. Cances, A. Omahen, M. Masseroni, M. J. Ruckriegel, C. Adam, C. Tong, R. Garreis, J. D. Gerber, W. Huang, L. Gächter, K. Watanabe, T. Taniguchi, T. Ihn, and K. Ensslin, Spin-valley locked excited states spectroscopy in a one-particle bilayer graphene quantum dot, *Nature Communications* **15**, 10.1038/s41467-024-54121-4 (2024).

[55] M. Cramer, M. B. Plenio, S. T. Flammia, R. Somma, D. Gross, S. D. Bartlett, O. Landon-Cardinal, D. Poulin, and Y.-K. Liu, Efficient quantum state tomography, *Nature Communications* **1**, 10.1038/ncomms1147 (2010).

[56] D. Marković, A. Mizrahi, D. Querlioz, and J. Grollier, Physics for neuromorphic computing, *Nature Reviews Physics* **2**, 499–510 (2020).

[57] A. Mehonic, D. Ielmini, K. Roy, O. Mutlu, S. Kvatincky, T. Serrano-Gotarredona, B. Linares-Barranco, S. Spiga, S. Savel'ev, A. G. Balanov, N. Chawla, G. Desoli, G. Malavenna, C. Monzio Compagnoni, Z. Wang, J. J. Yang, S. G. Sarwat, A. Sebastian, T. Mikolajick, S. Slezacek, B. Noheda, B. Dieny, T.-H. A. Hou, A. Varri, F. Brückerhoff-Plückelmann, W. Pernice, X. Zhang, S. Pazos, M. Lanza, S. Wiefels, R. Dittmann, W. H. Ng, M. Buckwell, H. R. J. Cox, D. J. Mannion, A. J. Kenyon, Y. Lu, Y. Yang, D. Querlioz, L. Hutin, E. Vianello, S. S. Chowdhury, P. Mannocci, Y. Cai, Z. Sun, G. Pedretti, J. P. Strachan, D. Strukov, M. Le Gallo, S. Ambrogio, I. Valov, and R. Waser, Roadmap to neuromorphic computing with emerging technologies, *APL Materials* **12**, 10.1063/5.0179424 (2024).

[58] D. Kudithipudi, C. Schuman, C. M. Vineyard, T. Pandit, C. Merkel, R. Kubendran, J. B. Aimone, G. Orchard, C. Mayr, R. Benosman, J. Hays, C. Young, C. Bartolozzi, A. Majumdar, S. G. Cardwell, M. Payvand, S. Buckley, S. Kulkarni, H. A. Gonzalez, G. Cauwenberghs, C. S. Thakur, A. Subramoney, and S. Furber, Neuromorphic computing at scale, *Nature* **637**, 801–812 (2025).

[59] S. Khandelwal, N. Brunner, and G. Haack, Signatures of liouvillian exceptional points in a quantum thermal machine, *PRX Quantum* **2**, 040346 (2021).

[60] S. Khandelwal and G. Blasi, Emergent liouvillian exceptional points from exact principles (2024), arXiv:2409.08100.

[61] J. A. Gyamfi, Fundamentals of quantum mechanics in liouville space, *European Journal of Physics* **41**, 10.1088/1361-6404/ab9fd (2020).

[62] J. Bourgeois, G. Blasi, S. Khandelwal, and G. Haack, Finite-time dynamics of an entanglement engine: Current, fluctuations and kinetic uncertainty relations, *Entropy* **26**, 497 (2024).

[63] G. Blasi, R. R. Rodríguez, M. Moskalets, R. López, and G. Haack, Quantum kinetic uncertainty relations in mesoscopic conductors at strong coupling (2025), arXiv:2505.13200 [cond-mat.mes-hall].

End matter

Proof of Eqs. (6) and (7)

We proceed by inductance to demonstrate the main identity connecting the current superoperator and the occupation-number operators, Eq. (6) in the main text.

Let us first consider a single qubit connected to a single reservoir, assuming the validity of the definition of the current superoperator defined below Eq. (29). We can therefore write for any operator \hat{u} :

$$\begin{aligned} \text{Tr}[\mathcal{I}_j \hat{u}] &= \text{Tr}[\gamma_j^+ \hat{\sigma}_j^+ \hat{u} \hat{\sigma}_j^- - \gamma_j^- \hat{\sigma}_j^- \hat{u} \hat{\sigma}_j^+] \\ &= \gamma_j^+ \text{Tr}[\hat{\sigma}_j^- \hat{\sigma}_j^+ \hat{u}] - \gamma_j^- \text{Tr}[\hat{\sigma}_j^+ \hat{\sigma}_j^- \hat{u}] \\ &= \text{Tr}[(\gamma_j^+ - \Gamma_j \hat{n}_j) \hat{u}], \end{aligned} \quad (15)$$

where we have used the properties of linearity and permutation under the trace, as well as the commutation relations $\{\hat{\sigma}_j^+, \hat{\sigma}_j^-\} = \mathbb{I}$. Inverting this relation, we obtain:

$$\text{Tr}[\hat{n}_j \hat{u}] = \text{Tr}\left[\left(\frac{\gamma_j^+ - \mathcal{I}_j}{\Gamma_j}\right) \hat{u}\right]. \quad (16)$$

For m distinct qubits coupled to m distinct reservoirs (defining the set P), we assume the validity of the above relation:

$$\text{Tr}[\hat{n}_P \hat{u}] = \text{Tr}\left[\prod_{j \in P} \left(\frac{\gamma_j^+ - \mathcal{I}_j}{\Gamma_j}\right) \hat{u}\right]. \quad (17)$$

For $m+1$ qubits, we add an additional qubit labeled j_0 , that does not belong to the set P . Therefore, $[\hat{n}_{j_0}, \hat{n}_P] = 0$ and $[\sigma_{\pm}^{j_0}, \hat{n}_P] = 0$. This allows to write:

$$\text{Tr}[\hat{n}_{j_0} \hat{n}_P \hat{u}] = \text{Tr}\left[\left(\frac{\gamma_{j_0}^+ - \mathcal{I}_{j_0}}{\Gamma_{j_0}}\right) \hat{n}_P \hat{u}\right] = \text{Tr}\left[\hat{n}_P \left(\frac{\gamma_{j_0}^+ - \mathcal{I}_{j_0}}{\Gamma_{j_0}}\right) \hat{u}\right], \quad (18)$$

Applying the iteration hypothesis to the operator $\left(\frac{\gamma_{j_0}^+ - \mathcal{I}_{j_0}}{\Gamma_{j_0}}\right) \hat{u}$, we obtain for the set $P' = P \cup \{j_0\}$:

$$\text{Tr}[\hat{n}_{P'} \hat{u}] = \text{Tr}\left[\prod_{j \in P'} \left(\frac{\gamma_j^+ - \mathcal{I}_j}{\Gamma_j}\right) \hat{u}\right]. \quad (19)$$

Finally, taking the k -th derivative and considering $\hat{u} = \hat{\rho}$ lead to Eq. (6). Equation (7) is obtained after a simple algebraic manipulation by inserting the definition of the current moment $I_P^{(k)}$ given by Eq. (2) into Eq. (6). This ends the proof of these two main equations establishing the connection between Krylov subspaces generated by the Lindbladian and transport quantities.

Detailed equations for the two-qubit paradigmatic example

In the case of a two-qubit system, Eq. (7) applies for $P = \{L\}, \{R\}, \{L, R\}$, yielding

$$p_{L,k}(t) = \frac{1}{\Gamma_L} (\delta_{k,0} \gamma_L^+ - I_L^{(k)}(t)) \quad (20a)$$

$$p_{R,k}(t) = \frac{1}{\Gamma_R} (\delta_{k,0} \gamma_R^+ - I_R^{(k)}(t)) \quad (20b)$$

$$p_{LR,k}(t) = \frac{1}{\Gamma_L \Gamma_R} (\delta_{k,0} \gamma_L^+ \gamma_R^+ - \gamma_R^+ I_L^{(k)}(t) - \gamma_L^+ I_R^{(k)}(t) + I_{LR}^{(k)}(t)). \quad (20c)$$

For $k = 0$, these elements correspond to occupation numbers of the qubit states. Recalling that the number operators \hat{n}_j act as the projector $|1\rangle\langle 1|$ on qubit j and as the identity elsewhere, we have

$$p_{L,0} = \langle \hat{n}_L \rangle \equiv n_L = r_{10} + r_{11} \quad (21a)$$

$$p_{R,0} = \langle \hat{n}_R \rangle \equiv n_R = r_{01} + r_{11} \quad (21b)$$

the occupation numbers of the left and right qubits respectively, and

$$p_{LR,0} = \langle \hat{n}_L \hat{n}_R \rangle = r_{11} \quad (22)$$

the occupation number of the doubly-occupied state. By introducing the current cross-correlation function $S_{LR}(t) = I_{LR}(t) - I_L(t)I_R(t)$, the above equations can

be rewritten as:

$$n_L(t) = r_{10}(t) + r_{11}(t) = \frac{\gamma_L^+ - I_L(t)}{\Gamma_L}, \quad (23a)$$

$$n_R(t) = r_{01}(t) + r_{11}(t) = \frac{\gamma_R^+ - I_R(t)}{\Gamma_R}, \quad (23b)$$

$$r_{11}(t) = \frac{S_{LR}(t)}{\Gamma_L \Gamma_R} + \frac{\gamma_L^+ - I_L(t)}{\Gamma_L} \frac{\gamma_R^+ - I_R(t)}{\Gamma_R}. \quad (23c)$$

A straightforward calculation leads to the set of Eq. (66) for the populations of $\hat{\rho}$.

For $k \geq 1$, the $p_{P,k}$ correspond to the k -th time derivatives of the $p_{P,k}$, such that $p_{L,k}(t) = n_L^{(k)}(t)$, $p_{R,k}(t) = n_R^{(k)}(t)$ and $p_{LR,k}(t) = r_{11}^{(k)}(t)$. The evolution of the two-qubit system being given by Eqs. (10) and (11), we have

$$\dot{n}_L(t) = \gamma_L^+ - \Gamma_L n_L + 2g_{\text{res}} \text{Im}(\alpha) + 2g_{\text{off}} \text{Im}(\beta), \quad (24a)$$

$$\dot{n}_R(t) = \gamma_R^+ - \Gamma_R n_R - 2g_{\text{res}} \text{Im}(\alpha) + 2g_{\text{off}} \text{Im}(\beta). \quad (24b)$$

Simple algebra then yields the expressions of the imaginary parts of the off-diagonal coherences, $\text{Im}(\alpha)(t)$ and $\text{Im}(\beta)(t)$, Eq. (12) in the main text.

Similarly, we have

$$\begin{aligned} \ddot{n}_L(t) = & -\Gamma_L (\gamma_L^+ - \Gamma_L n_L) \\ & + 2g_{\text{res}}^2 (n_R - n_L) + 2g_{\text{off}}^2 (r_{00} - r_{11}) \\ & - \left(\frac{\tilde{\Gamma}}{2} + \Gamma_L \right) (2g_{\text{res}} \text{Im}(\alpha) + 2g_{\text{off}} \text{Im}(\beta)) \\ & + 2g_{\text{res}} \delta \text{Re}(\alpha) + 2g_{\text{off}} E \text{Re}(\beta), \end{aligned} \quad (25a)$$

$$\begin{aligned} \ddot{n}_R(t) = & -\Gamma_R (\gamma_R^+ - \Gamma_R n_R) \\ & - 2g_{\text{res}}^2 (n_R - n_L) + 2g_{\text{off}}^2 (r_{00} - r_{11}) \\ & - \left(\frac{\tilde{\Gamma}}{2} + \Gamma_R \right) (-2g_{\text{res}} \text{Im}(\alpha) + 2g_{\text{off}} \text{Im}(\beta)) \\ & - 2g_{\text{res}} \delta \text{Re}(\alpha) + 2g_{\text{off}} E \text{Re}(\beta), \end{aligned} \quad (25b)$$

with $\delta = \varepsilon_L - \varepsilon_R$ the energy detuning between the qubits, $E = \varepsilon_L + \varepsilon_R + U$ the energy of the doubly-occupied state $|11\rangle$, $\tilde{\Gamma} = \Gamma_L + \Gamma_R + 2\Gamma_z$ the total dissipation strength and $\Gamma_z = \gamma_L^z + \gamma_R^z$ the total pure dephasing strength. After some simplifications, Eq. (6) for $j = L, R$ and $k = 2$ provides the transport-based QST expressions for the real parts of the off-diagonal coherences:

$$-4g_{\text{res}} \delta \text{Re}(\alpha) = \left(\frac{\ddot{I}_L}{\Gamma_L} + \dot{I}_L - \frac{\ddot{I}_R}{\Gamma_R} - \dot{I}_R \right) + \frac{\tilde{\Gamma}}{2} \left(\frac{\dot{I}_L}{\Gamma_L} + I_L - \frac{\dot{I}_R}{\Gamma_R} - I_R \right) + 4g_{\text{res}}^2 \left(\frac{I_L - \gamma_L^+}{\Gamma_L} - \frac{I_R - \gamma_R^+}{\Gamma_R} \right), \quad (26a)$$

$$-4g_{\text{off}} E \text{Re}(\beta) = \left(\frac{\ddot{I}_L}{\Gamma_L} + \dot{I}_L + \frac{\ddot{I}_R}{\Gamma_R} + \dot{I}_R \right) + \frac{\tilde{\Gamma}}{2} \left(\frac{\dot{I}_L}{\Gamma_L} + I_L + \frac{\dot{I}_R}{\Gamma_R} + I_R \right) + 4g_{\text{off}}^2 \left(\frac{I_L - \gamma_L^+}{\Gamma_L} + \frac{I_R - \gamma_R^+}{\Gamma_R} + 1 \right). \quad (26b)$$

Steady-state transport-based QST for two qubits

In the case of the two-qubit system, considering a zero off-resonant inter-qubit interaction ($g_{\text{off}} = 0$), of specific

interest in the context of entanglement generation from

out-of-equilibrium currents [29, 33], current conservation implies $I_L^{ss} = -I_R^{ss} \equiv I^{ss}$ and only the α -coherence remains finite (see also [62]). Its real and imaginary parts can be reconstructed through the equations:

$$2g_{\text{res}}\text{Im}(\alpha)^{ss} = -I^{ss}, \quad (27\text{a})$$

$$2g_{\text{res}}\delta\text{Re}(\alpha)^{ss} = 2g_{\text{res}}^2 \left(\frac{\gamma_L^+}{\Gamma_L} - \frac{\gamma_R^+}{\Gamma_R} \right) - \left(\frac{\tilde{\Gamma}}{2} + \frac{4g_{\text{res}}^2}{\Gamma_L\Gamma_R} \frac{\Gamma}{2} \right) I^{ss}. \quad (27\text{b})$$

Interestingly, the first equation corresponds to previously-established connection between steady-state currents and non-zero coherences in this setup. While it was derived analytically in the steady-state regime in previous works [33, 35, 62], this work provides a transport interpretation of this connection, bringing a complete and fundamental reason to its existence (see Supp. Mat. for further insights on intra-system transport [41]). Additionally, the measurement of the steady-state current averages and correlations allows us to determine the pure dephasing strength, $\Gamma_z = \frac{1}{2}(\tilde{\Gamma} - \Gamma)$ with $\Gamma = \Gamma_L + \Gamma_R$, if the other dynamics parameters are known. Indeed, taking the time derivative of Eq. (26b) and its steady-state limit yields

$$\left(\left(\frac{\tilde{\Gamma}}{2} \right)^2 + \frac{g_{\text{res}}^2\Gamma\tilde{\Gamma}}{\Gamma_L\Gamma_R} + \delta^2 \right) I^{ss} = 2g_{\text{res}}^2\tilde{\Gamma} \left(\frac{\gamma_L^+}{\Gamma_L} - \frac{\gamma_R^+}{\Gamma_R} \right), \quad (28)$$

from which $\tilde{\Gamma}$ can be extracted.

Appendix A: Methodology

Local master equation

Our model of the system's evolution is based on the local Lindblad master equation [33, 37–40] assessing the quantum dynamics of N qubits, among which M are individually tunnel-coupled to M distinct thermal reservoirs at equilibrium (with $\hbar = k_B = 1$ throughout the text):

$$\dot{\rho} = \mathcal{L}\hat{\rho} = \mathcal{L}_S\hat{\rho} + \sum_{j=1}^M (\gamma_j^+ \mathcal{D}[\hat{\sigma}_+^{(j)}] + \gamma_j^- \mathcal{D}[\hat{\sigma}_-^{(j)}])\hat{\rho}, \quad (29)$$

with \mathcal{L}_S the Lindblad superoperator setting the evolution of the system in the absence of the M reservoirs and $\mathcal{D}[\hat{A}] \bullet \equiv \hat{A} \bullet \hat{A}^\dagger - (\hat{A}^\dagger \hat{A} \bullet + \bullet \hat{A}^\dagger \hat{A})/2$ the dissipator associated to the operator \hat{A} . Denoting γ_j the bare reservoir-qubit coupling rate at side j and $n_{F/B}^j(\epsilon) = (1 \pm e^{(\epsilon - \mu_j)/T_j})^{-1}$ the probability distribution of bath j (respectively for a fermionic or bosonic reservoir), the in- and out-going coupling rates γ_j^+ , γ_j^- are given by

$$\gamma_j^+ = \gamma_j n_{F/B}^j(\epsilon_j) \quad \text{and} \quad \gamma_j^- = \gamma_j (1 \mp n_{F/B}^j(\epsilon_j)), \quad (30)$$

with the upper sign for fermions and the lower one for bosons. Here, the probability distribution of the reservoir j is evaluated at the bare energy ϵ_j of its associated qubit, while T_j and μ_j denote the reservoir's temperature and chemical potential.

The local Lindblad master equation correctly captures the dynamics of the reduced density operator for the N -qubit system when the reservoir-qubit and inter-qubit couplings are small with respect to the other energy scales, and when the reservoirs can be considered as Markovian. For a two-qubit system with Hamiltonian $\hat{H}_S = \varepsilon_L \hat{n}_L + \varepsilon_R \hat{n}_R + U \hat{n}_L \hat{n}_R + (g_{\text{res}} \hat{\sigma}_+^{(L)} \hat{\sigma}_-^{(R)} + g_{\text{off}} \hat{\sigma}_+^{(L)} \hat{\sigma}_+^{(R)} + h.c.)$, where U , g_{res} and g_{off} respectively set on-site, resonant (particle-conserving) and off-resonant (particle-non-conserving) interactions and are supposed real and positive without loss of generality, such conditions consist in [33, 40, 43]:

$$\gamma_L, \gamma_R \ll T_L, T_R, |\epsilon_L - \mu_L|, |\epsilon_R - \mu_R| \quad \text{and} \quad g_{\text{res}}, g_{\text{off}} \lesssim \gamma_j. \quad (31)$$

If the assumption of weak inter-qubit coupling is not satisfied, the global Master equation provides a more accurate description of the system's evolution, see for instance [42]. While the relation between the measurements of current superoperators and occupation-number operators will be accordingly modified, there is no conceptual difference with the case treated in this work.

Arnoldi iteration

The Arnoldi iteration [45] provides the construction of an orthonormal basis for Krylov spaces of open quantum systems [46]: from an operator \hat{u} , it generates an orthonormal set $\{\hat{v}_0, \dots, \hat{v}_k, \dots\}$ from the application of the Lindbladian \mathcal{L}^\dagger on \hat{u} , such that

$$\text{span}(\hat{v}_0, \dots, \hat{v}_k) = \text{span}(\hat{u}, \dots, \mathcal{L}^{\dagger k} \hat{u}). \quad (32)$$

The algorithm is initialized by defining $\hat{v}_0 = \hat{u}/\|\hat{u}\|$. Then, is iteratively defined, for $k = 1, 2, \dots$:

- $\hat{u}_k = \mathcal{L}^\dagger \hat{v}_{k-1}$, the result of the action of the Lindbladian \mathcal{L}^\dagger onto the Arnoldi operator \hat{v}_{k-1} ;
- $\tilde{u}_k = \hat{u}_k - \sum_{n=0}^{k-1} \langle \hat{v}_n, \hat{u}_k \rangle \hat{v}_n$, the projection of \hat{u}_k on the complement subspace of $\text{span}(\hat{v}_0, \dots, \hat{v}_{k-1})$;
- If $\|\tilde{u}_k\| > 0$, then $\hat{v}_k = \tilde{u}_k/\|\tilde{u}_k\|$. Otherwise, stop the iteration.

For a quantum system with finite dimension, the iteration stops at some index $k = K$ that corresponds to the dimension of the Krylov space of \hat{u} .

For the transport-based QST, the Arnoldi iteration provides a practical tool for constructing states from transport measurements. Given a Lindbladian \mathcal{L} , we numerically compute for each $P \subseteq \{1, \dots, M\}$, the Arnoldi basis

$\{\hat{v}_0^P, \dots, \hat{v}_{K_P-1}^P\}$ of the Krylov subspace $\mathcal{K}_P = \text{span}\{\mathcal{L}^{\dagger k} \hat{n}_P \mid k \in \mathbb{N}\}$. Because of overlaps between the different Krylov subspaces, the sum of these subspaces, $\mathcal{K} = \sum_P \mathcal{K}_P$, has its dimension $K_{tot} \leq \sum_P K_P$. To perform QST over the states in \mathcal{K} , one has to choose an ensemble of indexes $\{L_P \leq K_P \mid P \subseteq \{1, \dots, M\}\}$ such that

$$\sum_P L_P = K \quad \text{and} \quad \text{span}(\hat{v}_k^P, P \subseteq \{1, \dots, M\}, k \leq L_P) = \mathcal{K}. \quad (33)$$

Then measuring the $I_P^{(k)}$ for $P \subseteq \{1, \dots, M\}$ and $k \leq L_P$ determines the parts of the system's state in \mathcal{K} in an optimal way.

Appendix B: QST Completeness and Lindbladian spectrum

In this section, we analyze how symmetries, and more generally spectral properties of the Lindblad superoperator, affect the completeness of the transport-based QST of a general qubit system. We note λ_i , $\hat{\rho}_i$ and $\hat{\sigma}_i$ respectively the eigenvalues, the right and left eigen-operators of the Lindbladian, $\mathcal{L}\hat{\rho}_i = \lambda_i \hat{\rho}_i$ and $\mathcal{L}^\dagger \hat{\sigma}_i = \lambda_i^* \hat{\sigma}_i$. For a non-hermitian Lindbladian, the eigen-operators are not in general orthonormal, $\langle \hat{\rho}_i, \hat{\rho}_j \rangle \neq \delta_{ij}$. Still, the left and right eigen-operators are bi-orthogonal with respect to the Hilbert-Schmidt product, $\langle \hat{\sigma}_i, \hat{\rho}_j \rangle = \text{Tr}[\hat{\sigma}_i^\dagger \hat{\rho}_j] = \delta_{ij}$.

If the Lindbladian is diagonalisable, the left and right eigen-operators each form a complete basis for the Hilbert space. The Krylov operators $\mathcal{L}^{\dagger k} \hat{n}_P$ are then set by:

$$\mathcal{L}^{\dagger k} \hat{n}_P = \sum_{i=1}^n \lambda_i^{*k} \langle \hat{\rho}_i, \hat{n}_P \rangle \hat{\sigma}_i, \quad (34)$$

with n the dimension of the operator Hilbert space. The corresponding set of equations for $k = 0$ to $n-1$ when evaluating on the state $\hat{\rho}(t)$ can be combined into the matrix equation

$$\vec{I} = \Lambda^* V \vec{S}, \quad (35)$$

with \vec{I} the vector of state coefficients that can be obtained from current measurements,

$$\vec{I} = (\text{Tr}[\mathcal{L}^{\dagger k} \hat{n}_P \hat{\rho}(t)])_{0 \leq k \leq n-1} = (p_{k,P})_{0 \leq k \leq n-1},$$

Λ the Vandermonde matrix of the Lindbladian eigenvalues,

$$\Lambda = \begin{pmatrix} 1 & 1 & \dots & 1 \\ \lambda_1 & \lambda_2 & \dots & \lambda_n \\ \vdots & \vdots & & \vdots \\ \lambda_1^{n-1} & \lambda_2^{n-1} & \dots & \lambda_n^{n-1} \end{pmatrix},$$

V the diagonal matrix of the overlaps between the occupation number operator \hat{n}_P and the eigen-operators $\hat{\rho}_i$,

$$V = \text{Diagonal}(\langle \hat{\rho}_i, \hat{n}_P \rangle, 1 \leq i \leq n),$$

and \vec{S} the coefficients of $\hat{\rho}(t)$ in the eigenbasis $\{\hat{\rho}_i\}$,

$$\vec{S} = (\text{Tr}[\hat{\sigma}_i \hat{\rho}])_{1 \leq i \leq n}.$$

Note that Λ is invertible if and only if the λ_i 's are all different, and V if the elements $\langle \hat{\rho}_i, \hat{n}_P \rangle$ are non-zero.

In the case of all eigenvalues λ_i of the Lindbladian being different, the latter decomposition shows that the Krylov space \mathcal{K}_P generated by \hat{n}_P contains exactly the left eigen-operators $\hat{\sigma}_i$ for which $\langle \hat{\rho}_i, \hat{n}_P \rangle \neq 0$. This implies that we may have complete QST when every right eigen-operator $\hat{\rho}_i$ has non-vanishing overlap with at least one occupation-number operator, i.e. $\mathcal{K} = \text{span}(\hat{\sigma}_i \mid \exists P \subseteq \{1, \dots, M\}, \langle \hat{\rho}_i, \hat{n}_P \rangle \neq 0)$.

If the Lindbladian's spectrum $\mathcal{S}(\mathcal{L})$ has some degeneracies, i.e. eigenvalues that correspond to several eigenvectors, then the Krylov space of \hat{n}_P changes for $\mathcal{K}_P = \text{span}(\sum_{\lambda_i=\lambda} \langle \hat{\rho}_i, \hat{n}_P \rangle \hat{\sigma}_i \mid \lambda \in \mathcal{S}(\mathcal{L}))$. The number of vectors in \mathcal{K}_P has reduced compared to the case of no degeneracy in the Lindbladian's spectrum, reducing as much the amount of states that can be determined from the measurements of the $I_P^{(k)}$, $k \in \mathbb{N}$. This loss could however be recovered overall by

considering several subsets P_s , such that the $\sum_{\lambda_i=\lambda} \langle \hat{\rho}_i, \hat{n}_{P_s} \rangle \hat{\sigma}_i$ would be linearly independent.

If the Lindbladian is non-diagonalizable, i.e. in the case of an exceptional point [59, 60], some eigenvalues and their eigen-operators both coalesce. The Lindbladian can then be written in a Jordan canonical form. For example, in the case of an exceptional point of order 2 for the eigenvalue λ_{EP} , we can define through a Jordan chain the normalized right eigen-operators $\hat{\rho}_{EP}^{(1)}$ and $\hat{\rho}_{EP}^{(2)}$ such that $(\mathcal{L} - \lambda_{EP})\hat{\rho}_{EP}^{(1)} = 0$ and $(\mathcal{L} - \lambda_{EP})\hat{\rho}_{EP}^{(2)} = A\hat{\rho}_{EP}^{(1)}$ with $A \in \mathbb{C}^*$. The left eigen-operators $\hat{\sigma}_i$ and $\hat{\sigma}_{EP}^{(r)}$ are constructed biorthogonal with the right eigen-operators. The Krylov operators $\mathcal{L}^{\dagger k} \hat{n}_P$ then read:

$$\mathcal{L}^{\dagger k} \hat{n}_P = \sum \lambda_i^{*k} c_i^P \hat{\sigma}_i + \lambda_{EP}^{*k} c_{EP}^{(2)} \hat{\sigma}_{EP}^{(2)} + (\lambda_{EP}^{*k} c_{EP}^{(1)} + k \lambda_{EP}^{*k-1} A^* c_{EP}^{(2)}) \hat{\sigma}_{EP}^{(1)} \quad (36)$$

with $c_i^P = \langle \hat{\rho}_i, \hat{n}_P \rangle$ and $c_{EP}^{(r)} = \langle \hat{\rho}_{EP}^{(r)}, \hat{n}_P \rangle$ for $r = 1, 2$. Assuming that the eigenvalues other than λ_{EP} have no degeneracy, the Krylov space \mathcal{K}_P exactly contains the eigenvectors $\hat{\sigma}_i$ such that $c_i^P \neq 0$, plus $\hat{\sigma}_{EP}^{(1)}$ (respectively $\hat{\sigma}_{EP}^{(2)}$) if $c_{EP}^{(1)} \neq 0$ or $c_{EP}^{(2)} \neq 0$ (resp. if $c_{EP}^{(2)} \neq 0$). Compared to the case of a diagonalizable Lindbladian, we have increased the completeness of the transport-based QST since the condition on measuring the state $\hat{\rho}_{EP}^{(1)}$ has been loosened while those for other eigen-operators have remain identical.

Appendix C: Study of the two-qubit system

Vectorization of the open quantum system

To gain a more complete understanding of the results presented in the main text on the two-qubit case, we perform row-wise vectorization [61], which acts on the density matrix written in the Fock basis as

$$\hat{\rho} = \sum p_{n_L n_R}^{m_L m_R} |n_L n_R\rangle \langle m_L m_R| \longrightarrow |\rho\rangle\rangle = \sum p_{n_L n_R}^{m_L m_R} |m_L m_R\rangle \otimes |n_L n_R\rangle, \quad (37)$$

and transforms superoperators into operators as

$$\mathcal{A}\hat{\rho} = \hat{A}_1 \hat{\rho} \hat{A}_2 \longrightarrow \mathbf{A} = (\hat{A}_1 \otimes \hat{A}_2^T) |\rho\rangle\rangle. \quad (38)$$

This representation is specially convenient for analytics and numerics, as the quantum objects can be easily created using Kroenecker products.

For the sake of our analysis, we hereafter move to the basis where the density matrix

$$\rho = \begin{pmatrix} r_{00} & v & x & \beta \\ v^* & r_{01} & \alpha & y \\ x^* & \alpha^* & r_{10} & z \\ \beta^* & y^* & z^* & r_{11} \end{pmatrix} \quad (39)$$

is described by the vector

$$\vec{\rho} = (r_{00}, r_{01}, r_{10}, r_{11}, \text{Im}(\alpha), \text{Re}(\alpha), \text{Im}(\beta), \text{Re}(\beta), \text{Im}(x), \text{Re}(x), \text{Im}(y), \text{Re}(y), \text{Im}(v), \text{Re}(v), \text{Im}(z), \text{Re}(z))^T. \quad (40)$$

Structure of the Lindbladian

Following this vectorization, the evolution equation resumes to a linear differential equation:

$$\partial_t \vec{\rho}(t) = \mathbf{L} \vec{\rho}(t) \quad (41)$$

with the Lindblad matrix $\mathbf{L} = \mathbf{L}_{\text{unit}} + \mathbf{L}_{\text{diss}}$ made of two components: a unitary-evolution matrix

$$\mathbf{L}_{\text{unit}} = -i(H_S \otimes \mathbb{I}_4 - \mathbb{I}_4 \otimes H_S^T) \quad (42)$$

and a dissipative-evolution matrix $\mathbf{L}_{\text{diss}} = \sum_{j=L,R} (\mathbf{L}_j^+ + \mathbf{L}_j^- + \mathbf{L}_j^z)$, with

$$\mathbf{L}_j^s = \gamma_j^s (\sigma_s^{(j)} \otimes \sigma_s^{(j)}) - \frac{1}{2} (\sigma_s^{(j)\dagger} \sigma_s^{(j)} \otimes \mathbb{I}_4 + \mathbb{I}_4 \otimes (\sigma_s^{(j)\dagger} \sigma_s^{(j)})^T) \quad (43)$$

for $s = R, L, z$. The matrices \mathbf{L}_{unit} and \mathbf{L}_{diss} may be decomposed into 16 blocks of dimension 4×4 , corresponding to the different components of the dynamics:

i) The evolution set by the dissipative terms, induced by the presence of reservoirs and of pure dephasing, is captured by the block-diagonal matrix

$$\mathbf{L}_{\text{diss}} = \begin{pmatrix} \mathbf{L}_{\text{diss}}^{\text{pop}} & & & \\ & \mathbf{L}_{\text{diss}}^{\alpha\beta} & & \\ & & \mathbf{L}_{\text{diss}}^{xy} & \\ & & & \mathbf{L}_{\text{diss}}^{vz} \end{pmatrix} \quad (44)$$

with the subspace matrices

$$\mathbf{L}_{\text{diss}}^{\text{pop}} = \begin{pmatrix} -(\gamma_L^+ + \gamma_R^+) & \gamma_R^- & \gamma_L^- & 0 \\ \gamma_R^+ & -(\gamma_L^+ + \gamma_R^-) & 0 & \gamma_L^- \\ \gamma_L^+ & 0 & -(\gamma_L^- + \gamma_R^+) & \gamma_R^- \\ 0 & \gamma_L^+ & \gamma_R^+ & -(\gamma_L^- + \gamma_R^-) \end{pmatrix} \quad \mathbf{L}_{\text{diss}}^{xy} = -\frac{\Gamma_L + 2\gamma_L^z}{2} \mathbb{I}_4 + \begin{pmatrix} -\gamma_R^+ & 0 & \gamma_R^- & 0 \\ 0 & -\gamma_R^+ & 0 & \gamma_R^- \\ \gamma_R^+ & 0 & -\gamma_R^- & 0 \\ 0 & \gamma_R^+ & 0 & -\gamma_R^- \end{pmatrix} \quad (45)$$

$$\mathbf{L}_{\text{diss}}^{\alpha\beta} = -\frac{\tilde{\Gamma}}{2} \mathbb{I}_4 \quad \mathbf{L}_{\text{diss}}^{vz} = -\frac{\Gamma_R + 2\gamma_R^z}{2} \mathbb{I}_4 + \begin{pmatrix} -\gamma_L^+ & 0 & \gamma_L^- & 0 \\ 0 & -\gamma_L^+ & 0 & \gamma_L^- \\ \gamma_L^+ & 0 & -\gamma_L^- & 0 \\ 0 & \gamma_L^+ & 0 & -\gamma_L^- \end{pmatrix} \quad (46)$$

Here, $\Gamma_r = \gamma_r^+ + \gamma_r^-$ for $r = L, R$, $\Gamma = \Gamma_L + \Gamma_R$, $\Gamma_z = \gamma_L^z + \gamma_R^z$ and $\tilde{\Gamma} = \Gamma + \Gamma_z$. \mathbf{L}_{diss} exponentially suppresses the coherences, as expected, while generating coupling between the populations and between pairs of coherences, (x, y) and (v, z) .

ii) On-site energies and interaction, $\hat{H}_{\text{on-site}} = \epsilon_L \hat{n}_L + \epsilon_R \hat{n}_R + U \hat{n}_L \hat{n}_R$, yield a superoperator which is also block diagonal in this basis:

$$\mathbf{L}_{\text{on-site}} = \begin{pmatrix} \mathbf{L}_{\text{on-site}}^{\text{pop}} & & & \\ & \mathbf{L}_{\text{on-site}}^{\alpha\beta} & & \\ & & \mathbf{L}_{\text{on-site}}^{xy} & \\ & & & \mathbf{L}_{\text{on-site}}^{vz} \end{pmatrix} \quad (47)$$

with the subspace matrices

$$\mathbf{L}_{\text{on-site}}^{\text{pop}} = 0 \quad \mathbf{L}_{\text{on-site}}^{xy} = \begin{pmatrix} 0 & \epsilon_L & & \\ -\epsilon_L & 0 & & \\ & 0 & \epsilon_L + U & \\ & & -(\epsilon_L + U) & 0 \end{pmatrix} \quad (48)$$

$$\mathbf{L}_{\text{on-site}}^{\alpha\beta} = \begin{pmatrix} 0 & \delta & & \\ -\delta & 0 & & \\ 0 & E & & \\ -E & 0 & & \end{pmatrix} \quad \mathbf{L}_{\text{on-site}}^{vz} = \begin{pmatrix} 0 & \epsilon_R & & \\ -\epsilon_R & 0 & & \\ & 0 & \epsilon_R + U & \\ & & -(\epsilon_R + U) & 0 \end{pmatrix} \quad (49)$$

It couples real and imaginary parts of the coherences.

iii) The other interactions between the two qubits, set by the Hamiltonian $\hat{H}_{\text{int}} = g_{\text{res}} (\hat{\sigma}_+^{(L)} \hat{\sigma}_-^{(R)} + \hat{\sigma}_-^{(L)} \hat{\sigma}_+^{(R)}) + g_{\text{off}} (\hat{\sigma}_+^{(L)} \hat{\sigma}_+^{(R)} + \hat{\sigma}_-^{(L)} \hat{\sigma}_-^{(R)})$, correspond to the superoperator:

$$\mathbf{L}_{\text{on-site}} = \begin{pmatrix} 0 & -2\mathbf{L}_{\text{int}}^{(1)T} & 0 & 0 \\ \mathbf{L}_{\text{int}}^{(1)} & 0 & 0 & 0 \\ 0 & 0 & 0 & -\mathbf{L}_{\text{int}}^{(2)T} \\ 0 & 0 & \mathbf{L}_{\text{int}}^{(2)} & 0 \end{pmatrix} \quad (50)$$

with

$$\mathbf{L}_{\text{int}}^{(1)} = \begin{pmatrix} 0 & g_{\text{res}} & -g_{\text{res}} & 0 \\ 0 & 0 & 0 & 0 \\ 0 & 0 & 0 & 0 \\ 0 & 0 & 0 & 0 \end{pmatrix} + \begin{pmatrix} 0 & 0 & 0 & 0 \\ 0 & 0 & 0 & 0 \\ g_{\text{off}} & 0 & 0 & -g_{\text{off}} \\ 0 & 0 & 0 & 0 \end{pmatrix}, \quad (51)$$

$$\mathbf{L}_{\text{int}}^{(2)} = \begin{pmatrix} 0 & g_{\text{res}} & 0 & 0 \\ -g_{\text{res}} & 0 & 0 & 0 \\ 0 & 0 & -g_{\text{res}} & 0 \\ 0 & 0 & g_{\text{res}} & 0 \end{pmatrix} + \begin{pmatrix} 0 & 0 & 0 & -g_{\text{off}} \\ 0 & 0 & -g_{\text{off}} & 0 \\ 0 & g_{\text{off}} & 0 & 0 \\ g_{\text{off}} & 0 & 0 & 0 \end{pmatrix}. \quad (52)$$

The resonant part of the inter-qubit interaction couples the populations and the dynamics of the first off-diagonal coherence, $\alpha(t)$, while the off-resonant part couples the populations and the dynamics of the second off-diagonal coherence, $\beta(t)$. They also interconnect the (x, y) and (v, z) pairs of coherences.

Generalization towards complete QST

To perform complete QST of a full density matrix, one needs to consider a Hamiltonian with additional elements - for example, local drives on the qubits, $\hat{H}_{\text{drive}} := f_L(\sigma_+^{(L)} + \sigma_-^{(L)}) + f_R(\sigma_+^{(L)} + \sigma_-^{(L)})$ with f_L and f_R real amplitudes of the drives. The matrix of the associated superoperator, decomposed into 4×4 blocks, reads:

$$\mathbf{L}_{\text{drive}} = \begin{pmatrix} 0 & 0 & -2\mathbf{L}_{\text{drive}}^{(L1)T} & 0 \\ 0 & 0 & 0 & -\mathbf{L}_{\text{drive}}^{(L2)T} \\ \mathbf{L}_{\text{drive}}^{(L1)} & 0 & 0 & 0 \\ 0 & \mathbf{L}_{\text{drive}}^{(L2)} & 0 & 0 \end{pmatrix} + \begin{pmatrix} 0 & 0 & 0 & -2\mathbf{L}_{\text{drive}}^{(R1)T} \\ 0 & 0 & -\mathbf{L}_{\text{drive}}^{(R2)T} & 0 \\ 0 & \mathbf{L}_{\text{drive}}^{(R2)} & 0 & 0 \\ \mathbf{L}_{\text{drive}}^{(R1)} & 0 & 0 & 0 \end{pmatrix} \quad (53)$$

with

$$\mathbf{L}_{\text{drive}}^{(L1)} = \begin{pmatrix} f_L & 0 & -f_L & 0 \\ 0 & f_L & 0 & -f_L \\ 0 & 0 & 0 & 0 \end{pmatrix} \quad \mathbf{L}_{\text{drive}}^{(L2)} = \begin{pmatrix} 0 & -f_L & 0 & f_L \\ -f_L & 0 & -f_L & 0 \\ f_L & 0 & f_L & 0 \end{pmatrix} \quad (54)$$

$$\mathbf{L}_{\text{drive}}^{(R1)} = \begin{pmatrix} f_R & -f_R & 0 & 0 \\ 0 & 0 & f_R & -f_R \\ 0 & 0 & 0 & 0 \end{pmatrix} \quad \mathbf{L}_{\text{drive}}^{(R2)} = \begin{pmatrix} 0 & -f_R & 0 & f_R \\ f_R & 0 & -f_R & 0 \\ -f_R & 0 & f_R & 0 \end{pmatrix} \quad (55)$$

The drive on qubit L (respectively on qubit R) couples the evolution of the populations and with the one of the (x, y) (resp. (v, z)) coherence pair of coherences, and of (α, β) and (v, z) (resp. (x, y)).

The resulting total Hamiltonian $\hat{H}_{\text{tot}} = \hat{H}_{\text{on-site}} + \hat{H}_{\text{int}} + \hat{H}_{\text{drive}}$ is a full matrix:

$$\hat{H}_{\text{tot}} = \begin{pmatrix} 0 & f_R & f_L & g_{\text{off}} \\ f_R & \epsilon_R & g_{\text{res}} & f_L \\ f_L & g_{\text{res}} & \epsilon_R & f_R \\ g_{\text{off}} & f_L & f_R & E \end{pmatrix} \quad (56)$$

with $E = \epsilon_R + \epsilon_L + U$ the energy of the doubly-occupied state. In this case, all coherences can be constructed from Krylov states of the occupation-number operators, and the transport-based QST is informally complete. For example, the first derivatives of the occupation numbers read:

$$\dot{n}_L(t) = \gamma_L^+ - \Gamma_L n_L + 2g_{\text{res}} \text{Im}(\alpha(t)) + 2g_{\text{off}} \text{Im}(\beta(t)) + f_L \text{Im}(x(t) + y(t)), \quad (57)$$

$$\dot{n}_R(t) = \gamma_R^+ - \Gamma_R n_R - 2g_{\text{res}} \text{Im}(\alpha(t)) + 2g_{\text{off}} \text{Im}(\beta(t)) + f_R \text{Im}(v(t) + z(t)). \quad (58)$$

The imaginary part of the α and β coherences cannot be determined from $(\dot{I}_L, I_L, \dot{I}_R, I_R)$ anymore. To get a closed set of equations on the coherences, one needs to consider additional equations, obtained similarly from higher time-derivatives.

Appendix D: Current correlation functions

Definitions

The quantum jumps of excitations tunneling into (respectively out of) the system, induced by the presence of reservoir j , are described within the local Lindblad master equation formalism by the superoperators

$$\mathcal{L}_j^+ := \gamma_j^+ \sigma_+^{(j)} \bullet \sigma_-^{(j)}, \quad (59)$$

$$\mathcal{L}_j^- := \gamma_j^- \sigma_-^{(j)} \bullet \sigma_+^{(j)}. \quad (60)$$

It was recently derived in [43], using a full-counting statistics approach, that within this formalism, the correlation function $S_{j_1 j_2}(t_1, t_2)$ between the currents in reservoir j_1 at time t_1 and j_2 at time t_2 equals to

$$\begin{aligned} S_{j_1 j_2}(t_1, t_2) := & \delta_{j_1, j_2} \delta(t_1 - t_2) \text{Tr}\{\mathcal{A}_{j_1} \hat{\rho}(t_1)\} \\ & + \Theta(t_1 - t_2) \text{Tr}\{\mathcal{I}_{j_1} e^{\mathcal{L}(t_1 - t_2)} \mathcal{I}_{j_2} \hat{\rho}(t_2)\} \\ & + \Theta(t_2 - t_1) \text{Tr}\{\mathcal{I}_{j_2} e^{\mathcal{L}(t_2 - t_1)} \mathcal{I}_{j_1} \hat{\rho}(t_1)\} \\ & - \text{Tr}\{\mathcal{I}_{j_1} \hat{\rho}(t_1)\} \text{Tr}\{\mathcal{I}_{j_2} \hat{\rho}(t_2)\}, \end{aligned} \quad (61)$$

with $\mathcal{I}_j := \mathcal{L}_j^+ - \mathcal{L}_j^-$ and $\mathcal{A}_j := \mathcal{L}_j^+ + \mathcal{L}_j^-$ the current and activity superoperators associated to reservoir j . The first term of this expression, the dynamical activity $A_{j_1}(t) = \text{Tr}[\mathcal{A}_{j_1} \hat{\rho}(t)]$, is present only for instantaneous auto-correlation functions and describes the rate of jumps occurring at the interface with the reservoir j , regardless of their direction [43, 62, 63].

Instantaneous auto-correlation functions

The instantaneous ($t_1 = t_2 = t$) auto-correlation functions are formally given by:

$$S_{j,j}(t, t) = \delta(0) A_j(t) + \text{Tr}[\mathcal{I}_j^2 \hat{\rho}(t)] - I_j(t)^2. \quad (62)$$

The presence of the δ -distribution in this definition calls for a special care when manipulating $S_{j,j}(t, t)$. This is usually done by working in the frequency domain, analyzing measurements performed over a time window rather than at a fixed time. As for the transport-based QST, we note that the instantaneous auto-correlation functions do not provide further information on the quantum state than the current averages, since

$$\text{Tr}[\mathcal{I}_j^2 \hat{\rho}(t)] - I_j(t)^2 = -\Gamma_j(\gamma_j^+(1 - n_j(t))^2 + \gamma_j^- n_j(t)^2), \quad (63)$$

$$A_j(t) = \gamma_j^+(1 - n_j(t)) + \gamma_j^- n_j(t). \quad (64)$$

For this reason, we believe the instantaneous auto-correlation functions would not be relevant for transport-based QST.

Two-time correlation functions

In general, the superoperator $e^{\mathcal{L}(t_1 - t_2)}$ corresponds to a very complex matrix, whose analytical expression is not to be given here. Still, for two-qubit systems, one may explore the information contained in the two-time correlation functions by studying the matrices

$$\begin{aligned} \mathcal{I}_L \rho(t) &= \begin{pmatrix} -\gamma_L^- r_{10}(t) & -\gamma_L^- z(t) & 0 & 0 \\ -\gamma_L^- z^*(t) & -\gamma_L^- r_{11}(t) & 0 & 0 \\ 0 & 0 & \gamma_L^+ r_{00}(t) & \gamma_L^+ v(t) \\ 0 & 0 & \gamma_L^+ v^*(t) & \gamma_L^+ r_{01}(t) \end{pmatrix} \\ \mathcal{I}_R \rho(t) &= \begin{pmatrix} -\gamma_R^- r_{01}(t) & 0 & -\gamma_R^- y(t) & 0 \\ 0 & \gamma_R^+ r_{00}(t) & 0 & \gamma_R^+ x(t) \\ -\gamma_R^- y^*(t) & 0 & -\gamma_R^+ r_{11}(t) & 0 \\ 0 & \gamma_R^+ x^*(t) & 0 & \gamma_R^+ r_{10}(t) \end{pmatrix} \end{aligned}$$

where r_{ij} , v , x , y and z are elements of the density matrix ρ , as introduced in Eq. (39).

Importantly, the coherences $\alpha(t)$ and $\beta(t)$ are absent from these matrices, yielding that no information about these coherences can be obtained from $S_{j_1 j_2}(t_1, t_2)$ itself. This aspect justifies the need for other transport quantities, like current-average time-derivatives, to perform complete transport-based QST.

Appendix E: How to access the system's parameters

Main result

The QST protocol introduced in this work relies on the precise knowledge of the system dynamics parameters. If the system's Hamiltonian \hat{H}_S or the rates of the dissipation processes are not known quantitatively, it is first necessary to measure them. An extension of the transport-based QST protocol precisely allows one to estimate these dynamics parameters from additional transport observables, higher-order time derivatives of the current averages. In Table II, we summarize all necessary transport quantities to be measured to achieve such determination for the two-qubit system presented in the main text, depending on the completeness of \hat{H}_S .

Condition on \hat{H}_S	Dynamics parameters	Transport quantities
	$g_{\text{res}}, g_{\text{off}}, \delta, E, \Gamma_z$	$I_L^{(0)}(t_i), \dots, I_L^{(3)}(t_i)$ and $I_R^{(0)}(t_i), \dots, I_R^{(3)}(t_i)$ for $i = 1, \dots, 5$
$\delta = 0$ $E = 0$	$g_{\text{res}}, g_{\text{off}}$	$I_L^{(0)}(t_i), \dots, I_L^{(2)}(t_i)$ and $I_R^{(0)}(t_i), \dots, I_R^{(2)}(t_i)$ for $i = 1, 2, 3$
$g_{\text{off}} = 0$	$g_{\text{res}}, \delta, \Gamma_z$	$I_L^{(0)}(t_i), \dots, I_L^{(3)}(t_i)$ or $I_R^{(0)}(t_i), \dots, I_R^{(3)}(t_i)$ for $i = 1, 2, 3$

TABLE II. Summary of the transport-based dynamics probing, when all Hamiltonian and pure-dephasing parameters are missing experimental data.

Formal argument

The operators $\mathcal{L}^{\dagger k} \hat{n}_P$, for $k \in \mathbb{N}$ and $P \subseteq \{1, \dots, M\}$, are not all linearly independent. A set of current moments $I_P^{(k)}$, with several pairs (k, P) , can thus contain redundant information on the system's state, that can be used to probe the evolution parameters.

For example considering a single subset P , the Krylov space generated from \hat{n}_P has a finite dimension that we denote K_P : $\mathcal{K}_P = \text{span}(\hat{n}_P, \mathcal{L}^{\dagger} \hat{n}_P, \dots, \mathcal{L}^{\dagger K_P-1} \hat{n}_P)$. We thus have $\mathcal{L}^{\dagger K_P} \hat{n}_P = \sum_{k=0}^{K_P-1} c_k^P \mathcal{L}^{\dagger k} \hat{n}_P$ with $c_k^P \equiv \langle \mathcal{L}^{\dagger k} \hat{n}_P, \mathcal{L}^{\dagger K_P} \hat{n}_P \rangle = \text{Tr}[\hat{n}_P \mathcal{L}^{\dagger (K_P-k)} \hat{n}_P] = \text{Tr}[\mathcal{L}^{\dagger (K_P-k)} \hat{n}_P]$ being functions of the evolution parameters. Then measuring the current quantities $I_P(t), I'_P(t), \dots, I_P^{(K_P)}(t)$ provides the following equation on the c_k^P 's:

$$\sum_{k=0}^{K_P} c_k^P p_{P,k}(t) = 0, \quad (65)$$

with $c_{K_P}^P \equiv -1$, and the $p_{P,k}(t)$ given by the general QST expression in the main text. Measuring $I_P(t_i), I'_P(t_i), \dots, I_P^{(K_P)}(t_i)$ for different subsets P and different times t_i thus builds a set of conditions on the c_k^P 's that can be used to determine some evolution parameters.

Illustration with the two-qubit system

We illustrate this method with a two-qubit system.

In the simple case of two degenerate qubits, $\epsilon_L = \epsilon_R \equiv \epsilon$, and a resonant-only interaction, $g_{\text{off}} = 0$, the dynamics only couples the population $r_{00}, r_{01}, r_{10}, r_{11}$ to the imaginary coherence $i\text{Im}(\alpha)$. The transport-based QST's set of equations then resume to

$$r_{01}(t) = -\frac{S_{LR}(t)}{\Gamma_L \Gamma_R} - \frac{I_R(t) - \gamma_R^+}{\Gamma_R} \frac{I_L(t) + \gamma_L^-}{\Gamma}, \quad (66a)$$

$$r_{10}(t) = -\frac{S_{LR}(t)}{\Gamma_L \Gamma_R} - \frac{I_L(t) - \gamma_L^+}{\Gamma_L} \frac{I_R(t) + \gamma_R^-}{\Gamma}, \quad (66b)$$

$$r_{11}(t) = \frac{S_{LR}(t)}{\Gamma_L \Gamma_R} + \frac{I_L - \gamma_L^+}{\Gamma_L} \frac{I_R - \gamma_R^+}{\Gamma_R}, \quad (66c)$$

$$\text{Im}(\alpha) = \frac{1}{4g_{\text{res}}} \left(-\frac{\dot{I}_L}{\Gamma_L} - I_L + \frac{\dot{I}_R}{\Gamma_R} + I_R \right). \quad (66d)$$

The transport QST expression for $\text{Im}(\beta)$ is transformed in this case into the current conservation identity $\frac{\ddot{I}_L}{\Gamma_L} + I_L + \frac{\ddot{I}_R}{\Gamma_R} + I_R = 0$. Hence, the transport quantities needed for performing QST are simply $S_{LR}(t)$, $I_L(t)$, $I_R(t)$ and $\dot{I}_L(t)$. Further differentiating in time in Eq. (66d) yields

$$\frac{\ddot{I}_L}{\Gamma_L} + \dot{I}_L + \frac{\tilde{\Gamma}}{2} \left(\frac{\dot{I}_L}{\Gamma_L} + I_L \right) + 2g_{\text{res}}^2 \left(\frac{I_L - \gamma_L^+}{\Gamma_L} - \frac{I_R - \gamma_R^+}{\Gamma_R} \right) = 0. \quad (67)$$

If g_{res} is known *a priori*, the additional measurement of $\ddot{I}_L(t)$ at time t provides the value of $\tilde{\Gamma}$, and thus of the pure dephasing strength Γ_z . Otherwise, measuring \ddot{I}_L , \dot{I}_L , I_L and I_R at two different times t_1, t_2 determines both g_{res} and $\tilde{\Gamma}$. For error-prone measurements, the number of probe times may be increased to improve the fidelity of this protocol.

In the more general case studied in the main text, differentiating in time in the transport QST expressions for $\text{Re}(\alpha)$ and $\text{Re}(\beta)$ provides the equations:

$$0 = \Delta\ddot{\varphi}(t_i) + \tilde{\Gamma} \Delta\dot{\varphi}(t_i) + \left(\frac{\tilde{\Gamma}^2}{4} + \delta^2 \right) \Delta\varphi(t_i) + 4g_{\text{res}}^2 \Delta\dot{\chi}(t_i) + 2g_{\text{res}}^2 \tilde{\Gamma} \Delta\chi(t_i), \quad (68a)$$

$$0 = \ddot{\Phi}(t_i) + \tilde{\Gamma} \dot{\Phi}(t_i) + \left(\frac{\tilde{\Gamma}^2}{4} + E^2 \right) \Phi(t_i) + 4g_{\text{off}}^2 \dot{X}(t_i) + 2g_{\text{off}}^2 \tilde{\Gamma} X(t_i), \quad (68b)$$

with

$$\begin{aligned} \Delta\varphi(t) &= \varphi_L(t) - \varphi_R(t), & \Delta\chi(t) &= \chi_L(t) - \chi_R(t), \\ \Phi(t) &= \varphi_L(t) + \varphi_R(t), & X(t) &= \chi_L(t) + \chi_R(t), \\ \varphi_j(t) &= \frac{\dot{I}_j(t)}{\Gamma_j} + I_j(t), & \chi_j(t) &= \frac{I_j(t) - \gamma_j^+}{\Gamma_j}. \end{aligned}$$

In the case of an experimental set-up where all the Hamiltonian parameters are known, measuring $\ddot{I}_j(t)$ ($j = L$ or R), in addition to $\ddot{I}_j(t)$, $\dot{I}_j(t)$, $I_j(t)$, $I_L(t)$ and $I_R(t)$, determines the pure dephasing strength $\Gamma_z = \frac{1}{2}(\tilde{\Gamma} - \Gamma)$. Otherwise, first probing the four Hamiltonian parameters $g_{\text{res}}, g_{\text{off}}, \delta, E$ requires the measurement of $I_j^{(k)}(t_i)$ for $j = L, R$ and $k = 0, 1, 2, 3$ at, at least, four different times t_i .

Appendix F: Connection with current conservation laws

The tomography technique proposed in this work can be understood as a set of transport identities by introducing new transport quantities, internal to the bipartite system. In this section, we illustrate such link with the two-qubit system studied in the main text.

Extra-system transport

The current flowing from reservoir j to its connected qubit is captured in the Master-Equation formalism through the action of the superoperator $\mathcal{D}_j = \gamma_j^+ D[\hat{\sigma}_+^{(j)}] + \gamma_j^- D[\hat{\sigma}_-^{(j)}]$, and of the occupation-number operator \hat{n}_j , on the state. One can indeed derive that the qubit-reservoir current satisfies:

$$I_j(t) = \text{Tr}[\hat{n}_j \mathcal{D}_j \hat{\rho}(t)]. \quad (69)$$

Intra-system transport

The Hamiltonian part $\hat{H}_{\text{res}} = g_{\text{res}}(\sigma_+^{(L)}\sigma_-^{(R)} + \sigma_-^{(L)}\sigma_+^{(R)})$ preserves the total number of particle in the bipartite system,

$$\text{Tr}([\hat{n}_L + \hat{n}_R, \hat{H}_{\text{res}}] \hat{\rho}) = 0. \quad (70)$$

Its action generates particle transfers between the two qubits, inducing a current from the left to the right party equal, by definition, to

$$I_S := i \text{Tr}([\hat{n}_L, \hat{H}_{\text{res}}] \hat{\rho}) = -i \text{Tr}([\hat{n}_R, \hat{H}_{\text{res}}] \hat{\rho}). \quad (71)$$

For any generic density matrix, this internal current is determined by the α -coherence as

$$I_S = -2g_{\text{res}} \text{Im}(\alpha). \quad (72)$$

Meanwhile, the Hamiltonian term $\hat{H}_{\text{off}} = g_{\text{off}}(\sigma_+^{(L)}\sigma_+^{(R)} + \sigma_-^{(L)}\sigma_-^{(R)})$ preserves the particle imbalance between the two parties,

$$\text{Tr}([\hat{n}_L - \hat{n}_R, \hat{H}_{\text{off}}] \hat{\rho}) = 0. \quad (73)$$

Its action corresponds to a common particle production in the two qubits, given by

$$P_S := -i \text{Tr}([\hat{n}_L, \hat{H}_{\text{off}}] \hat{\rho}) = -i \text{Tr}([\hat{n}_R, \hat{H}_{\text{off}}] \hat{\rho}). \quad (74)$$

For any generic density matrix, this internal current is determined by the β -coherence as

$$P_S = 2g_{\text{off}} \text{Im}(\beta). \quad (75)$$

Current conservation laws

The time evolution of the local occupation number n_j for $j = L, R$ is set by

$$\dot{n}_j = \text{Tr}[\hat{n}_j \mathcal{L} \hat{\rho}] = \text{Tr}(\hat{n}_j \mathcal{D}_j \hat{\rho}) - i \text{Tr}([\hat{n}_j, H_I + H_J] \hat{\rho}), \quad (76)$$

Overall, we thus have the following transport identities:

$$\dot{n}_L = I_L - I_S + P_S, \quad (77a)$$

$$\dot{n}_R = I_R + I_S + P_S. \quad (77b)$$

Substituting n_j by its transport-based expression, one obtains the following equations on the internal and external transport quantities:

$$I_S = \frac{1}{2} \left(\frac{\dot{I}_L}{\Gamma_L} + I_L - \frac{\dot{I}_R}{\Gamma_R} - I_R \right), \quad (78a)$$

$$P_S = -\frac{1}{2} \left(\frac{\dot{I}_L}{\Gamma_L} + I_L + \frac{\dot{I}_R}{\Gamma_R} + I_R \right). \quad (78b)$$

This identity exactly corresponds to the QST expressions for the imaginary part of the coherences. Similarly, differentiating in time in Eq. (72)-(75), yields

$$\dot{I}_S = -\frac{\Gamma}{2}I_S - 2g_{\text{res}}\delta\text{Re}(\alpha) - 2g_{\text{res}}^2\left(\frac{I_L - \gamma_L^+}{\Gamma_L} - \frac{I_R - \gamma_R^+}{\Gamma_R}\right), \quad (79a)$$

$$\dot{P}_S = -\frac{\Gamma}{2}P_S + 2g_{\text{off}}E\text{Re}(\beta) + 2g_{\text{off}}^2\left(1 + \frac{I_L - \gamma_L^+}{\Gamma_L} + \frac{I_R - \gamma_R^+}{\Gamma_R}\right), \quad (79b)$$

which is a variant of the QST expressions for the real part of the coherences.

In conclusion, the tomography technique proposed in this work is based on the following set of correspondences: the current averages I_L and I_R directly determine the populations n_L and n_R ; their time derivatives \dot{I}_L and \dot{I}_R provides information on the imaginary coherences $\text{Im}(\alpha)$ and $\text{Im}(\beta)$ via the internal particle current and production I_S and P_S ; and finally, the second time derivatives \ddot{I}_L and \ddot{I}_R are linked with the the real coherences $\text{Re}(\alpha)$ and $\text{Re}(\beta)$ thanks to the time-derivation of I_S and P_S .

In the steady-state, current conservation identities in each qubit lead to the equations:

$$I_S^{ss} = (I_L^{ss} - I_R^{ss})/2, \quad (80a)$$

$$P_S^{ss} = -(I_R^{ss} + I_L^{ss})/2. \quad (80b)$$

The steady-state internal current I_S^{ss} is thus equal to the average current flowing from the left to the right reservoir, while the steady-state internal production P_S^{ss} counterbalances the average release of particles out of the system.

Appendix G: Transport-based entanglement measures

For the two-qubit system presented in the main text, initiated with an X-shaped density matrix, the concurrence is given at all time in terms of transport observables as:

$$\mathcal{C} = 2 \max\{0, |\alpha| - \sqrt{r_{00}r_{11}}, |\beta| - \sqrt{r_{01}r_{10}}\} \quad (81)$$

where

$$|\alpha| - \sqrt{r_{00}r_{11}} = \frac{1}{|2g_{\text{res}}|} \sqrt{\left(\varphi_L - \varphi_R\right)^2 + \frac{1}{\delta^2}(\dot{\varphi}_L - \dot{\varphi}_R + \frac{\tilde{\Gamma}}{2}(\varphi_L - \varphi_R) + 4g_{\text{res}}^2(\chi_L - \chi_R))^2} - \sqrt{\left(\frac{S_{LR}}{\Gamma_L\Gamma_R} + \chi_L\chi_R\right)\left(\frac{S_{LR}}{\Gamma_L\Gamma_R} + (\chi_L + 1)(\chi_R + 1)\right)} \quad (82)$$

and

$$|\beta| - \sqrt{r_{01}r_{10}} = \frac{1}{|2g_{\text{off}}|} \sqrt{\left(\varphi_L + \varphi_R\right)^2 + \frac{1}{E^2}(\dot{\varphi}_L + \dot{\varphi}_R + \frac{\tilde{\Gamma}}{2}(\varphi_L + \varphi_R) + 4g_{\text{off}}^2(\chi_L + \chi_R + 1))^2} - \sqrt{\left(\frac{S_{LR}}{\Gamma_L\Gamma_R} + \chi_L(\chi_R + 1)\right)\left(\frac{S_{LR}}{\Gamma_L\Gamma_R} + (\chi_L + 1)\chi_R\right)} \quad (83)$$

with $\varphi_j(t) = \frac{\dot{I}_j(t)}{\Gamma_j} + I_j(t)$ and $\chi_j(t) = \frac{I_j(t) - \gamma_j^+}{\Gamma_j}$. For the sake of clarity, time-dependence is implicit here.